

17 Quantitative Analysis of Renal Perfusion at Contrast-Enhanced US

EMILIO QUAIA

CONTENTS

- 17.1 Quantification of Perfusion by Doppler Techniques 255
 - 17.1.1 Spectral Doppler 256
 - 17.1.2 Power Doppler 256
- 17.2 Speckle Decorrelation 256
- 17.3 Quantitation of Renal Perfusion by Microbubble-Based Agents 256
 - 17.3.1 Intermittent High-Transmit-Power Technique 257
 - 17.3.2 Continuous Low-Transmit-Power Technique 257
- 17.4 Microbubble Injection 257
- 17.5 Objective Analysis of Echo Signal Intensity 257
- 17.6 Approximation by Mathematical Functions 259
 - 17.6.1 Wash-in/Wash-out Curves (Gamma Variate) 259
 - 17.6.2 Negative Exponential 260
 - 17.6.3 Sigmoid 260
 - 17.6.4 Other Mathematical Functions and Drawbacks in Mathematical Approximation 261
- 17.7 Clinical Applications of Renal Perfusion Quantitation 262
 - References 263

17.1 Quantification of Perfusion by Doppler Techniques

Tissue viability and function may be maintained only in the presence of adequate perfusion, which is tightly regulated to maintain factors such as nutrient delivery, gas exchange, and fluid balance. The ability to accurately quantify blood flow in solid organs is essential for a variety of reasons, including confirmation of organ or tissue viability, assessment of tumor ablation procedures, postoperative imaging where rejection or vascular complications may occur, and determination of the response to angiogenesis-modulating drugs.

Different parameters have to be considered in blood-flow quantitation. Firstly, the blood velocity

which corresponds to the speed of red blood cells (in centimeters per second) in the analyzed region. Secondly, the blood flow which is volume of blood passing in a section of tissue per unit of time (cubic centimeters per second), corresponding to the blood velocity \times section of perfused parenchymal tissue (expressed in square centimeters per second). The parenchymal perfusion corresponds to the parenchymal blood flow equalized for the volume or weight of the perfused parenchyma – or the amount of flow in a volume of tissue per unit of time – and it is expressed in $\text{cm}^3/\text{seconds}/\text{cm}^3$ or grams. Thirdly, the fractional vascular volume is an index of the physiological vascularity of a region and is the proportion of tissue occupied by blood.

Many imaging techniques, including radionuclide single-photon emission computed tomography (SPECT), ultrafast computed tomography (CT), magnetic resonance (MR) imaging, and positron emission tomography (PET), have been used to evaluate tissue blood flow; however, those techniques are not portable and expensive and present some inherent limitations such as the low availability and the patient exposition to irradiation or nuclear tracers.

The progressive improvement of microbubble and ultrasound (US) contrast-specific modes has determined the advent of a new non-invasive, portable, and relatively inexpensive modality for the assessment of tissue blood flow. Ultrasound provides excellent spatial resolution (<1 mm axially) and temporal resolution (240 Hz), which is even better than many other imaging modalities.

Microbubble-based contrast agents consist of stabilized microbubbles, filled by air or perfluorocarbon gas and covered by a peripheral shell of various composition and rigidity. Microbubbles remain entirely intravascular, mix uniformly with blood in the circulation, and possess the same intravascular rheology as red blood cells when injected intravenously. Perfluorocarbon or sulfur hexafluoride-filled agents (SCHNEIDER et al. 1995) present a strong harmonic behavior at low transmit power and are made by stabilized microbubbles of gases of high

E. QUAIA, MD
Assistant Professor of Radiology, Department of Radiology,
Cattinara Hospital, University of Trieste, Strada di Fiume 447,
34149 Trieste, Italy

molecular weight and low solubility in water which provides a longer persistence in the bloodstream than air-filled agents. Doppler, speckle decorrelation, and contrast-specific modes may be employed to assess flow (amount of blood passing per unit time, in milliliters per minute), perfusion (amount of flow in a volume of tissue per unit of time, in milliliters per minute per milligram), and fractional blood or vascular volume (tissue occupied by blood, in milliliters per milligram).

17.1.1

Spectral Doppler

Spectral Doppler may be employed to estimate the mean velocity of blood in a vessel, and if the cross-sectional area of the vessel is also measured, the product gives the mean flow rate. Due to difficulty of accurately measuring the vessel area and the time-averaged mean velocity, this estimation remains subject to serious errors and is operator dependent. Microbubble-based US contrast agents increase the intensity of spectral Doppler signal, which may be quantified via a sound card or a dedicated A-to-D audio converter to obtain time-intensity curves.

The mean transit time (MTT) may be derived from time-intensity curves (COSGROVE et al. 2001), through deconvolution mathematical procedures, and corresponds to the average persistence of a microbubble in the circulation of a region of tissue as it travels from an inflow to an outflow vessel. The MTT is also related to the renal blood flow (RBF) and fractional renal blood volume (RBV) by the central volume principle:

$$\text{RBF} = \frac{\text{RBV}}{\text{MTT}}.$$

17.1.2

Power Doppler

Power Doppler signals are log-compressed and proportional to the number of moving reflectors. After quantification and appropriate transformation (antilogging and correction for color post-processing), a power Doppler image should give a map of regional red-cell concentration and of fractional blood volume. After microbubble injection, a time-intensity curve can be obtained by analyzing the increase of signal intensity in a region of interest (ROI). Fractional blood volume could be calculated by dividing the area under the time-intensity

curve obtained from a parenchymal region by that obtained from a vascular region of interest, while perfusion may be quantified by measuring the concentration of microbubbles in vivo.

17.2

Speckle Decorrelation

Because US is a coherent imaging method, the amplitude of the received US signal fluctuates as a result of the relative spatial arrangement of sub-resolution scatterers, which generate speckle (RUBIN et al. 1999). The phenomenon manifests in B-mode images as fluctuations in time of the amplitude of speckle and is also observed in Doppler US as fluctuations of the signal amplitude. Decorrelation is caused by a change in the speckle pattern in a given sample volume determined by the dimensions of the US beam and the pulse length. Ideally, this speckle pattern change would be caused completely by fluid movement through the sample volume. Ultrasound gray-scale speckle decorrelation with bubble contrast agents may be useful for measuring blood flow in vivo (RUBIN et al. 1999).

17.3

Quantitation of Renal Perfusion by Microbubble-Based Agents

The accurate quantitation of parenchymal perfusion in solid organs is essential for confirmation of organ or tissue viability and determination of response to angiogenesis-modulating drugs. Presently, quantitation of organ perfusion can be performed non-invasively using dedicated US contrast-specific modes and microbubble-based contrast agents. A linear relation exists between microbubble concentration and the video signal intensity (CORREAS et al. 2000), which may be quantified by dedicated software to produce time-intensity curves.

With expanded use and development of microbubble-based contrast agents, a variety of innovative applications have been developed. The intravenous injection of microbubble-based contrast agents allows estimation of relative blood flow and fractional blood volume of the microvasculature in an ROI (WEI et al. 1998a). The first phenomenon which has to be elicited is microbubble destruction in the insonated tissue by applying a high-transmit

power train. The major factors influencing microbubble destruction are the transmit frequency and the transmit power which actually constitute the mechanical index (MI), inversely related to transducer frequency and directly to the transmit power and representing the amount of US energy being transmitted (WEI et al. 1997; CORREAS et al. 2002). After initial microbubble destruction, other trains of destructive high transmit power may be transmitted at increasing pulsing intervals or a continuous low transmit power may be employed to image tissue replenishment in real time. For both technique the fundamental assumption is that the relation between microbubble concentration and video intensity is linear up to the achievement of a plateau phase (CORREAS et al. 2000).

17.3.1

Intermittent High-Transmit-Power Technique

By setting up an infusion of microbubbles to produce a steady blood concentration, the bubbles in a imaged slice may be destroyed by applying a train of high-transmit power frames. After microbubbles have been destroyed, the speed of tissue replenishment by microbubbles will depend on time interval between destructive pulses and the flow velocity of microbubbles. When the next destructive beam is applied, the intensity of the echoes depends on the number of bubbles that have flowed into the slice and so increased with longer intervals (WEI et al. 1998). If the process is repeated at a series of intervals, a time-intensity curve may be created and its slope is related to the speed of blood moving into the slice and the maximum level reached (the asymptote or plateau phase) relates to the vascular blood volume. This method is sensitive to relative movements between probe and the tissue because such movements expose a new slice of tissue that contains bubbles that have not been removed by the previous frame thus introducing errors.

17.3.2

Continuous Low-Transmit-Power Technique

Because US can destroy microbubbles, the change in echogenicity after tissue has been cleared of microbubbles can be imaged and quantified to obtain destruction-replenishment curve. This technique is also known as negative bolus since a void of microbubbles is created in the insonated tissue

which is refilled progressively by incoming bubbles (Fig. 17.1). With the recent introduction of bubble-specific imaging methods that operate at very low MI (0.08–0.21), such as power pulse inversion or pulse inversion mode, continuous interrogation can be performed without destroying bubbles in the slice so that the refill can be observed in real time and with much less likelihood of probe movements.

17.4

Microbubble Injection

In order for the concentration of microbubbles to be quantifiable, microbubbles have to be carefully administered to maintain concentrations in the circulation below the level of signal saturation. When a dilute solution of microbubbles is administered as a constant infusion, the concentration of microbubbles in circulation will reach a steady state (WEI et al. 1998). At steady state the number of microbubbles entering or leaving any microcirculatory unit is constant and depends on the flow rate. The bolus injection in a peripheral vein may be employed only to assess the mean organ transit time, while it must be avoided in contrast-specific modes since bolus dispersion in peripheral circulation do not allow assumption of a steady state in microcirculation. If microbubbles are injected directly as a discrete bolus in an artery supplying the organ, their mean transit rate through the parenchyma reflects the flow per unit volume (parenchymal blood flow/total artery blood flow), while the same relation does not apply if microbubbles are injected in a peripheral vein. Consequently to dispersion of microbubbles into the organ parenchyma, the parenchyma output function is wider than the input function. This problem can be partially solved by complex deconvolution mathematical procedures which are difficult and not always applicable.

17.5

Objective Analysis of Echo Signal Intensity

Determination of the degree of tissue contrast enhancement relies on accurate distinction between backscatterer signals originating from microbubbles and the intrinsic signal emanating from tissues which varies widely within the US sector for inhomogeneities of acoustic power and differences in

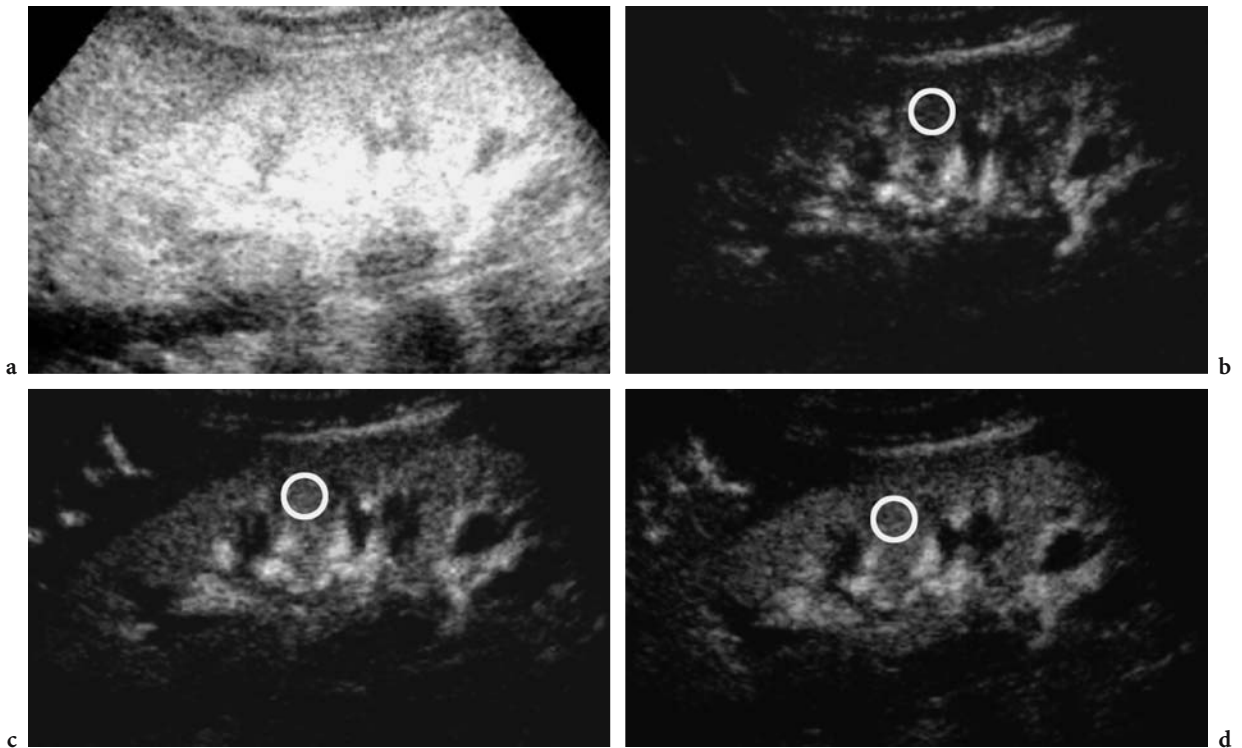


Fig. 17.1a–d. Progressive refilling of renal parenchyma at low acoustic power insonation after microbubble destruction. After image alignment and background subtraction, the echo signal intensity may be quantified by manually defined regions of interest (ROI) positioned in a region of renal parenchyma. A preliminary high acoustic power train of US pulses (a) destroy all the microbubbles comprised in the imaged slice of renal parenchyma. The progressive refilling of renal parenchyma by microbubbles is monitored at low acoustic power (b–d). The progressive higher echo signal intensity of renal parenchyma is determined by the progressive microbubble accumulation in the imaged slice.

attenuation and absorption of US energy by tissue. Direct visual assessment of the degree of contrast enhancement is the less accurate method.

Accurate quantitation of the degree of contrast enhancement requires assessment of the change in echo-signal intensity between the baseline and contrast-enhanced images. Digital image-processing techniques, such as image alignment, averaging, video densitometry, and background subtraction, are essential and may be performed by calculation software packages produced by the scanner manufacturers which have access to the raw data before applications of non-linear modifications (HDlab from Philips/ATL, Bothell, Wash.). These dedicated softwares allow to anti-log the gray-scale signals which are log-compressed for video presentation. Log-compressed video-intensity can be considered as:

$$10 * \log_{10} \left(\frac{I}{I_{\text{ref}}} \right),$$

where I is the acoustic intensity and I_{ref} is an intensity level determined through equipment gain.

The other possibility is to quantify directly the log-compressed video intensity of a digital cine clip. The log-compressed video-intensity does not provide a reliable quantification of microbubble signal, since several stages of post-processing in an ultrasound equipment for image video presentation, including log-compression, modify the original features of the signal. Moreover, the log-compressed video-intensity signal does provide quantification of what is displayed and used for qualitative clinical assessment (PHILLIPS and GARDNER 2004).

The echo signal intensity, linearized or log-compressed, may be quantified by positioning manually defined circular or rectangular ROIs in a region of renal parenchyma (Fig. 17.2), and by correlating time with the measured echo-signal video intensity in linear or logarithmic scale. Since the renal medulla presents a much lower perfusion (190 ml/min per 100 g) than the renal cortex (400 ml/min per 100 g; Fig. 17.2), it is preferable to encompass with a single manually defined ROI (Fig. 17.3) all the renal cortex excluding renal medulla.

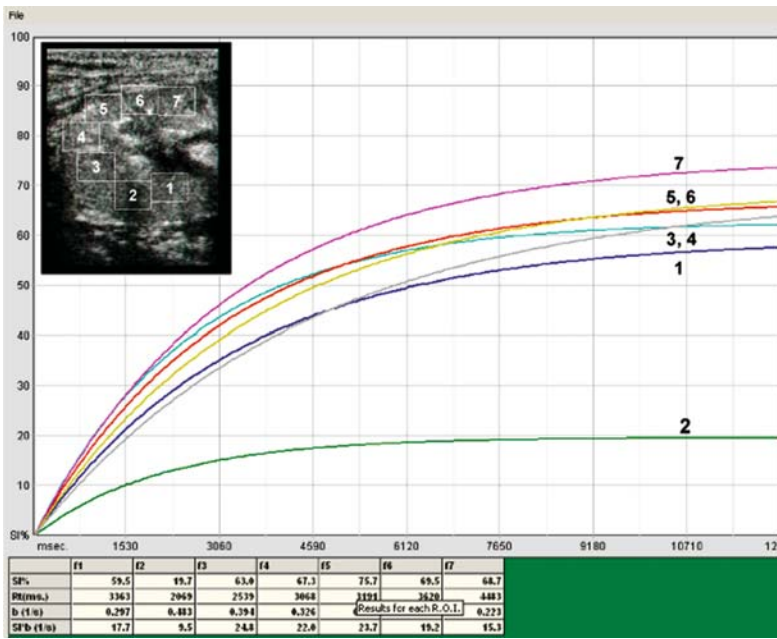


Fig. 17.2 Different refilling profile between different regions of interest positioned in renal cortex (regions 1 and 3–7) and one region of interest positioned in the renal medulla (region 2)

17.6 Approximation by Mathematical Functions

Different mathematical functions (Fig. 17.4) have been proposed to fit echo-signal intensity raw data vs time (LI and YANG 2003). The most employed is exponential negative ($A(1-e^{-\alpha t})$) based on a single-compartment model (WEI et al. 1998). The slope of the first ascending tract is related to microbubble velocity, while the plateau phase is related to fractional blood volume. This model, however, is based on continuous microbubble infusion into a single open compartment and is valid only if we assume that a constant number of microbubbles enters the region of interest per unit time. Recently, the exponential negative function was shown (LUCIDARME et al. 2003a) to present distortion toward a sigmoid curve if the percentage of bubbles destruction in the feeding vessels is not null. Even though both these functions could represent a reliable model, a wide variability between subjects exists: the first ascending tract of the curve presents a large interpolating error determined by the few available points, and both ascending and plateau phase tracts present large points dispersion.

17.6.1 Wash-in/Wash-out Curves (Gamma Variate)

The gamma variate (Fig. 17.4a) has the form $y=Ae^{-\alpha t}+C$, where A=the amplitude of the curve above

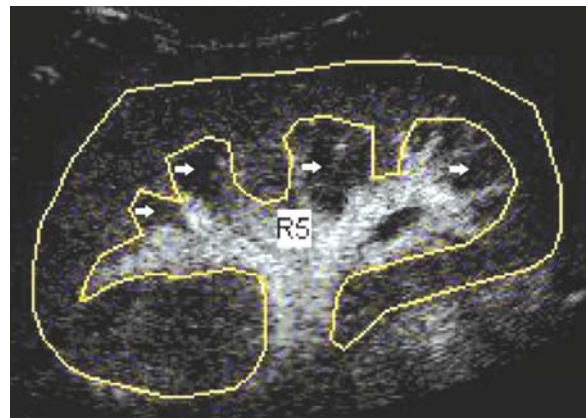


Fig. 17.3 It is possible to encompass with a single manually defined ROI all the renal parenchyma, excluding renal medulla (arrows), which presents a much lower perfusion value (190 ml/min per 100 g) if compared with renal cortex (400 ml/min per 100 g).

baseline, α =the initial slope of the curve, and C=the intensity at baseline (the zero crossing point of the y-axis). Wash in/out curves is generally described by a two-compartment filling and outflow model, which is mathematically represented by the gamma-variate function. Data from bolus injections of contrast, which have a distinct wash-in and wash-out phase, can be fit using this function. This protocol of injection is suitable for calculation of the MTT in an organ.

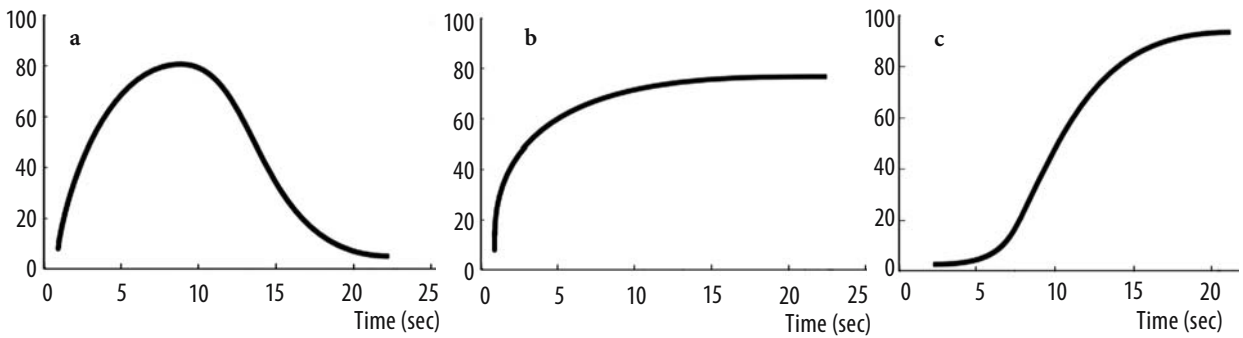


Fig. 17.4a–c. The most important mathematical models employed to fit echo-signal intensity vs time in renal parenchyma. The gamma variate (a) is suitable for intravenous bolus injection. When intravenous contrast infusion is employed the negative exponential (b) and the sigmoid (c) function are proposed to represent the refilling kinetic from microbubbles after destructive insonation.

17.6.2 Negative Exponential

The negative exponential function (Fig. 17.4b) has the form $y=A(1-e^{-\alpha t})+C$, where A =the amplitude of the curve above baseline, α =the initial slope of the curve, and C =the intensity at baseline (the zero crossing point of the y-axis). It is based on a single-compartment model (WEI et al. 1998, 2001) which has generally been proposed to fit time/intensity curves. According to this equation, the mean microbubble velocity in the microcirculation is related directly to α , the slope of the increasing function, and the plateau echo enhancement A correlates with the fractional blood volume (Fig. 17.5), provided that the microbubble destruction rate induced by the US field was considered null. Moreover, this exponential model is valid only if the concentration of microbubbles entering the ROI, immediately after the train of destructive pulses, is constant.

17.6.3 Sigmoid

SCHLOSSER et al. (2001) showed that different forms of function are observed for the replenishment curves from renal hilum vessels up to the renal cortex. The hilum replenishment exhibited an exponential that asymptotically approached a maximum, but the cortical replenishment showed a sigmoid curve. Recently, the exponential negative function was confirmed to present distortion toward a sigmoid curve (Fig. 17.4c), with a low initial slope that increases secondarily up to an inflexion point, if the percentage of bubble destruction in the ROI

feeding vessels is considered not null (LUCIDARME et al. 2003a).

$$C_n(t) = \frac{C_0}{(1+\tau\lambda)^n} \times \left[1 - \left(1 + \sum_{i=1}^{n-1} \frac{\beta^i t^i}{i!} \right) e^{-\beta t} \right]$$

and describes a curve with a low initial slope that increases secondarily to an inflexion point and is derived from the classic indicator dilution theory, by considering a series of subvolumes in the US field placed serially with respect to flow direction.

$C_n(t)$ is the refilling evolution of the microbubble concentration in the subvolume n , C_0 is the concentration of microbubbles in blood vessels that enter the ROI (number of microbubbles per liter), which is assumed to be constant with time, t is time, λ represents the fraction of microbubbles destroyed by the US beam per second, which is assumed to be constant,

$$\frac{1}{\tau} = \frac{F}{V_b}$$

where F is the rate of the inflow (equals to the rate of outflow) and V_b is the volume of flow in the ROI,

$$\text{and } \beta \text{ is } \frac{(1+\tau\lambda)}{\tau}.$$

In a sigmoid curve, the initial slope is theoretically equal to zero, and the slope measured at the inflexion point, even with a constant flow rate and a constant microbubble concentration in the circulation, decreases when the length of the path followed by the microbubbles in the US field increases before they reach the ROI. Consequently, microbubble velocity in the ROI estimated from the initial slope (α) of the refill curve, in the classic model described by an exponential function that approaches a maxi-



Fig. 17.5 Different mathematical parameters are calculated from negative exponential approximation of renal parenchyma refilling. The refilling time and the slope of the first ascending tract of the curve (b value) are related to the speed of the blood entering in the imaging slice. The peak of intensity in the plateau phase is related to the fractional blood volume in renal parenchyma. The flow is estimated by the product of the slope of the first ascending tract of the curve for the peak intensity value in the plateau phase.

mum, is not correct if microbubble destruction occurs in the feeding vessels.

17.6.4 Other Mathematical Functions and Drawbacks in Mathematical Approximation

Even though both negative exponential and sigmoid functions represent a reliable model to represent refilling kinetic in renal parenchyma, the first ascending tract of the curve is difficult to be fitted for the low availability of points which produces a large error of approximation (Fig. 17.6). As a further problem, the time-intensity curves present a large points dispersion both during the first ascending tract and the second plateau-phase tract of the curve (Fig. 17.6). A wide variability exists and further mathematical functions have been proposed to represent the refilling kinetic from microbubbles, such as the inverse negative exponential (LUCIDARME et al. 2003b) and the hyperbolic (KRIX et al. 2003).

Recently, a further mathematical model (QUAIA and TORELLI 2005) has been proposed which was derived from the biological models theory about progressive volume filling. The system was represented by a three-compartmental model, in which the large afferent vessels (segmentary, interlobar, and arciform arteries) represent the first compartment, the small cortical vessels (interlobular arteries and glomeruli) the second compartment ($K_{1,2}$ =transfer constant from the first to the second compartment),

and the small medullary vessels (the vasa recta capillaries) the third compartment ($K_{2,3}$ =transfer constant from the second to the third compartment).

Different variables are present in this model: (a) The direction of the vessels compared with the US beam. The refilling is almost instantaneous in the renal vessels which present a perpendicular direction to the US beam, while the refilling follows a complex kinetic in vessels parallel to the US beam; (b) Velocity of the blood in the vessels. Microbubble velocity entering the volume was considered as a multi-directional variable of control since the microbubbles refill the imaging volume from all the directions. The refilling is rapid in arterial vessels (segmentary, interlobar, and arciform), while it is

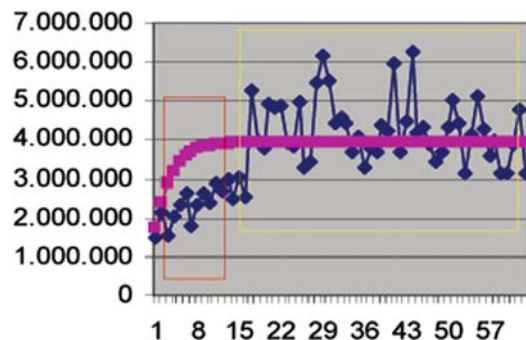


Fig. 17.6 The principal drawbacks in mathematical approximation of refilling kinetic in renal parenchyma. Red square=few points are available to approximate the first ascending tract of the curve; yellow square=the plateau phase presents a wide dispersion of data due to the variability of US signal.

more slow in the small cortical (interlobular, afferent, and efferent artery) and medullary (vasa recta) arteries and in the venous vessels; (c) Percentage of volume filled by the microbubbles. The imaged renal volume (thickness of the US beam ≈ 5 mm) was considered as a not conservative variable of state since the volume replenishment is dependent on the grade of filling.

A system of partial differential equations was derived including the velocity of volume replenishment, time, the volume percentage occupied by microbubbles, the percentage of microbubbles destroyed in the volume, and the percentage of microbubbles leaving the volume and not replaced.

17.7 Clinical Applications of Renal Perfusion Quantitation

Renal perfusion quantitation may be employed in different clinical situations with the aim of revealing a reduced perfusion of renal parenchyma.

Renal artery stenosis. One of the most important fields of application is the assessment of renal parenchyma perfusion in tight renal artery stenosis. The normally perfused kidney presents a higher slope of the first ascending tract of the curve and a higher value of gray-scale intensity at the plateau phase in comparison with the kidney presenting a tight renal artery stenosis (Fig. 17.7), revealing, respectively, a higher velocity in the blood entering the scanning plane and a higher fractional blood volume. These results seem encouraging, even though renal stenosis has to be tight ($>80\%$) for renal perfusion differences to become manifest at quantitative contrast-enhanced US.

Urinary obstruction. Contrast-enhanced US may depict changes in renal blood flow during acute obstruction, by revealing a lower area under the time-intensity curve during ureteral obstruction (CLAUDON et al. 1999).

Renal perfusion differences related to age. The renal perfusion is dependent on age, reflecting the changes in vessel structure. We analyzed (QUAIA et al. 2003) 50 normal volunteers (25 men and 25 women), 25 with age range between 27 and 48 years, and 25 between 61 and 80 years, with well-functioning native kidneys all without clinical and laboratory signs of renal failure after SonoVue peripheral intravenous slow infusion (4.8 ml at a flow rate of 4.0 ml/min) by automatic injector. After the blood concentration of microbubbles reached equilibrium, four high-transmit power (MI: 1.2–1.4) pulses were sent to destroy bubbles filling renal parenchyma in the imaged slice. By using a low-transmit power (MI: 0.06–0.08), the progressive replenishment of renal cortex was imaged in real time during apnea to avoid breathing-related movements for at least 6 s. Both kidneys were scanned.

The progressive refilling of renal cortex was quantified in linear scale after anti-log gray-scale transformation. Slope of the first ascending tract of the curve (α , 1/s) was related to the speed of blood (in centimeters per second) moving into the selected slice. To reduce variability between subjects due to the different signal gain, focal position, and anatomical features, the plateau values of renal cortex were equalized with those measured in the interlobar artery and the Ar/Ai (plateau intensity ratios in renal cortex, r; and interlobar renal artery, i) and AUCr/ AUCi (area-under-curve ratio in renal cortex, r; and interlobar renal artery, i) were related to the fractional blood volume. Since the fractional blood volume is related to the area of the capillary bed, the

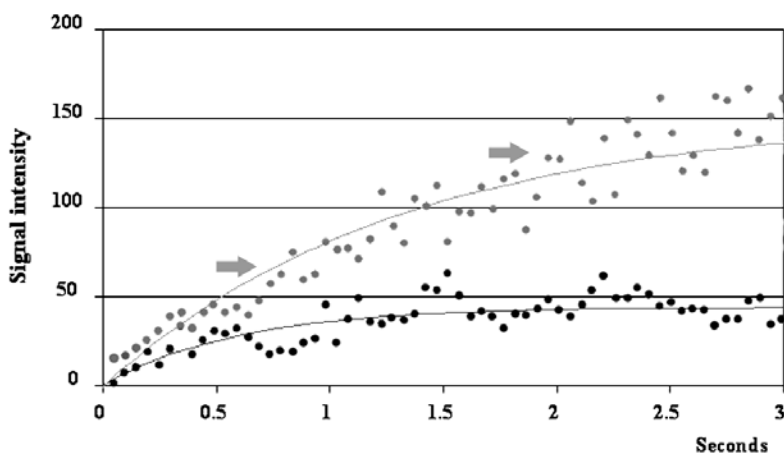


Fig. 17.7 Quantitation of renal perfusion through contrast-enhanced US, after sulfur hexafluoride-filled microbubble injection and at low acoustic power insonation. Difference in the refilling kinetics of renal parenchyma due to renal artery stenosis. The normally perfused kidney (arrows) presents a higher slope of the first ascending tract of the curve and a higher value of echo signal intensity at the plateau phase in comparison with the kidney which presents a tight renal artery stenosis (black points)

renal flow was related to the products $\alpha \times Ar/Ai$ and $\alpha \times AUCr/AUCi$ (Fig. 17.5).

No significant difference in cortical perfusion was found between the right and left kidneys in each volunteer, and between the cortical refilling time of group 1 to group 2 (4.4 ± 1.6 s vs 4.9 ± 1.3 s; $p=0.23$, Mann-Whitney U test). Despite that group 1 revealed an α value higher than group 2 (0.78 ± 0.16 vs 0.70 ± 0.43), the difference was not significant ($p=0.21$). Statistically significant difference was found between the Ar/Ai (0.048 ± 0.025 vs 0.016 ± 0.004 ; $p < 0.05$), $AUCr/AUCi$ (0.15 ± 0.19 vs 0.12 ± 0.14 ; $p < 0.05$), $\beta \times Ar/As$ (0.037 ± 0.017 vs 0.01 ± 0.006 ; $p < 0.05$) and $\alpha \times AUCr/AUCi$ (0.12 ± 0.20 vs 0.008 ± 0.09 ; $p < 0.05$) of group 1 vs group 2. These results showed that the principal differences in renal perfusion in different age groups can be quantitatively analyzed by contrast-enhanced US (Fig. 17.8).

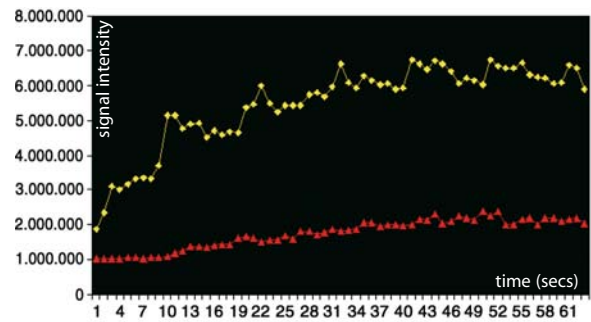


Fig. 17.8 Quantitation of renal perfusion through contrast-enhanced US, after sulfur hexafluoride-filled microbubble injection and at low acoustic power insonation. Difference in the refilling kinetics of renal parenchyma due to age. The kidney of a young volunteer (25 years of age) presents a higher slope of the first ascending tract of the curve (yellow) and a higher value of intensity at the plateau phase in comparison with the curve (red) obtained from a 65-year-old volunteer.

References

- Claudon M, Barnewolt CE, Taylor GA et al (1999) Renal blood flow in pigs: changes depicted with contrast-enhanced harmonic US imaging during acute urinary obstruction. *Radiology* 212:725–731
- Correas JM, Burns PN, Lai X, Qi X (2000) Infusion versus bolus of an ultrasound contrast agent: in vivo dose-response measurements of BR1. *Invest Radiol* 35:72–79
- Correas JM, Kurtisovski E, Bridal SF et al (2002) Optimizing an ultrasound contrast agent's stability using an in vitro measurement. *Invest Radiol* 37:672–679
- Cosgrove DO, Eckersley R, Blomley M, Harvey C (2001) Quantification of blood flow. *Eur Radiol* 11:1338–1344
- Krix M, Kiessling F, Farhan N et al (2003) A multivessel model describing replenishment kinetics of ultrasound contrast agent for quantification of tissue perfusion. *US Med Biol* 29:1421–1430
- Li PC, Ynag MJ (2003) Transfer function analysis of ultrasonic time-intensity measurements. *US Med Biol* 29:1493–1500
- Lucidarme O, Franchi-Abella S, Correas JM et al (2003a) Blood flow quantification with contrast-enhanced US: entrance in the section phenomenon – phantom and rabbit study. *Radiology* 228:473–479
- Lucidarme O, Kono Y, Corbeil J, Choi SH, Mattrey RF (2003b) Validation of ultrasound contrast destruction imaging for flow quantification. *Ultrasound Med Biol* 29:1697–1704
- Phillips P, Gardner E (2004) Contrast-agent detection and quantification. *Eur Radiol* 14 (Suppl 8):P4–P10
- Quaia E, Torelli L (2005) Proposal of an appropriate mathematical model representing replenishment kinetic of renal parenchyma after microbubbles destruction to assess numerical parameters related to perfusion [abstract]. European Congress of Radiology 2005
- Quaia E, Bertolotto M, Lubin E et al (2003) Evaluation of renal cortical perfusion by pulse inversion harmonic imaging with SonoVue: preliminary experience. *European Congress Radiology 2003. Eur Radiol* 13 [Suppl 1]
- Rubin JM, Fowlkes JB, Tuthill TA et al (1999) Speckle decorrelation flow measurement with B-mode US of contrast agent flow in a phantom and in rabbit kidney. *Radiology* 213:429–437
- Schlosser T, Pohl C, Veltmann C et al (2001) Feasibility of the FLASH-replenishment concept in renal tissue: Which parameters affect the assessment of the contrast replenishment? *Ultrasound Med Biol* 27:937–944
- Schneider M, Arditì M, Barrau MB et al (1995) BR1: a new ultrasonographic contrast agent based on sulfur hexafluoride-filled microbubbles. *Invest Radiol* 30:451–457
- Wei K, Skyba DM, Firsckhe C et al (1997) Interactions between microbubbles and ultrasound: in vitro and in vivo observations. *J Am Coll Cardiol* 29:1081–1088
- Wei K, Ananda R, Jayaweera AR et al (1998a) Quantification of myocardial blood flow with ultrasound-induced destruction of microbubbles administered as a constant venous infusion. *Circulation* 97:473–483
- Wei K, Jayaweera AR, Firoozan S et al (1998b) Basis for detection of stenosis using venous administration of microbubbles during myocardial contrast echocardiography: bolus or continuous infusion? *J Am Coll Cardiol* 32:252–260
- Wei K, Le E, Bin JP et al (2001) Quantification of renal blood flow with contrast-enhanced ultrasound. *J Am Coll Cardiol* 37:1135–1140

Cardiac Applications